RNA (1996), 2:535–550. Cambridge University Press. Printed in the USA.

Essential domains of the PRP21 splicing factor are implicated in the binding to PRP9 and PRP11 proteins and are conserved through evolution

JEAN-CHRISTOPHE RAIN,[1,*] ALAN M. TARTAKOFF,[2,*] ANGELA KRÄMER,[3] and PIERRE LEGRAIN[1]

[1] Laboratoire du Métabolisme des ARN, URA CNRS 1149, Département des Biotechnologies, Institut Pasteur, 28 rue du Dr Roux, 75724, Paris Cedex 15, France
[2] Institute of Pathology and Cell Biology Program, Case Western Reserve University, Cleveland, Ohio 44106, USA
[3] Département de Biologie Cellulaire, Université de Genève, CH-1211 Genève 4, Switzerland

ABSTRACT

The yeast Prp9p, Prp11p, Prp21p proteins form a multimolecular complex identified as the SF3a splicing factor in higher eukaryotes. This factor is required for the assembly of the prespliceosome. Prp21p interacts with both Prp9p and Prp11p, but the molecular basis of these interactions is unknown. Prp21p, its human homologue, and the so-called SWAP proteins share a tandemly repeated motif, the *surp* module. Given the evolutionary conservation and the role of SWAP proteins as splicing regulators, it has been proposed that *surp* motifs are essential for interactions between Prp21p and other splicing factors. In order to characterize functional domains of Prp21p and to identify potential additional functions of this protein, we isolated a series of heat-sensitive *prp21* mutants. Our results indicate that *prp21* heat-sensitive mutations are associated with defects in the interaction with Prp9p, but not with Prp11p. Interestingly, most heat-sensitive point mutants associate a strong splicing defect with a pre-mRNA nuclear export phenotype, as does the *prp9-1* heat-sensitive mutant. Deletion analyses led to the definition of domains required for viability. These domains are responsible for the interaction with Prp9p and Prp11p and are conserved through evolution. They do not include the most conserved *surp1* module, suggesting that the conservation of this motif in two families of proteins may reflect a still unknown function dispensable in yeast under standard conditions.

Keywords: Keywords: mutagenic PCR; plasmid shuffling; surp module; two-hybrid; yeast

INTRODUCTION

Nuclear introns are excised from mRNA precursors via two transesterification reactions that take place in a multicomponent complex, the spliceosome. The splicing mechanism is conserved from the yeast *Saccharomyces cerevisiae* to higher eukaryotes. Spliceosomes form on newly transcribed pre-mRNA by the addition of proteins and ribonucleoprotein particles (U1, U2, and U4/U6·U5 snRNPs, containing U1, U2, and U4, U5, and U6 snRNAs, respectively). Recognition of exon/intron boundaries as well as accurate and efficient splicing involve numerous interactions between individual splicing components. Base pairing interactions between snRNAs and the pre-mRNA or between individual snRNAs have been identified, as well as protein–RNA and protein–protein interactions (for review, see Moore et al., 1993; Legrain & Chanfreau, 1994; Madhani & Guthrie, 1994).

In vivo, the order of addition of splicing factors to the spliceosome has not yet been established, but splice site recognition and spliceosome assembly occur co-transcriptionally (for review see Spector, 1993). In the absence of efficient intron recognition and/or stable formation of splicing complexes, pre-mRNAs can be exported to the cytoplasm (Legrain & Rosbash, 1989). In vitro, the commitment of the pre-mRNA into the splicing pathway involves the interaction between the U1 snRNP and the 5′ splice site, which occurs simultaneously with recognition of the branchpoint region by an unknown factor (Legrain et al., 1988; Seraphin & Rosbash, 1989, 1991). The U2 snRNP then binds to the pre-mRNA in conjunction with additional proteins to

Reprint requests to: Pierre Legrain, Laboratoire du Métabolisme des ARN, URA CNRS 1149, Département des Biotechnologies, Institut Pasteur, 28 rue du Dr Roux, 75724, Paris Cedex 15, France; e-mail: plegrain@pasteur.fr.
* The first two authors contributed equally to this work.

form the prespliceosome, and finally, the spliceosome assembles after binding of the U4/U6·U5 snRNP as a triple particle (Behrens & Lührmann, 1991; Bennett et al., 1992; Utans et al., 1992). Many components essential for the formation of the prespliceosome have been characterized. In higher eukaryotes, four biochemical fractions, U2AF, SF1, and SF3a and SF3b are required for this step, in addition to the U1 and U2 snRNPs (Krämer & Utans, 1991; Brosi et al., 1993b). The functional U2 snRNP particle has been isolated as a 17S particle that includes the 12S U2 particle, SF3a, and SF3b (Brosi et al., 1993a). Components of SF3b interact with both the U2 snRNA and the pre-mRNA (Champion-Arnaud & Reed, 1994; Yan & Ares, 1995; K. Gröning, P. Grüter, & A. Krämer, in prep.).

In yeast, many heat-sensitive mutants have been isolated that are deficient for pre-mRNA splicing (prp mutants, for review see Rymond & Rosbash, 1992). The corresponding genes encode proteins of the splicing machinery as exemplified by specific phenotypes in vivo and/or in vitro that can be assigned to a given step of spliceosome assembly. Prp5p, Prp9p, Prp11p, Prp21p are early-acting factors, implicated in the addition of the U2 snRNP to the commitment complex (Abovich et al., 1990; Chapon & Legrain, 1992; Arenas & Abelson, 1993; Ruby et al., 1993; Wells & Ares, 1994). Genetic interactions between mutant forms of these proteins have been demonstrated and Prp9p, Prp11p, Prp21p, form a multimolecular complex (Legrain & Chapon, 1993; Legrain et al., 1993; Ruby et al., 1993). None of these proteins have been shown to bind to RNA. Very recently, a novel yeast polypeptide associated with the U2 snRNP particle and homologous to the human SF3b polypeptide SAP145 has been identified (Wells et al., 1996). A link with the U1 snRNP is likely because a genetic interaction has been found between *MUD2*, encoding a U1 snRNP-associated polypeptide, and *PRP11* (Abovich et al., 1994).

The importance of the Prp9p/Prp11p/Prp21p complex is suggested by its structural homology to human SF3a. Immunological cross-reactivity, sequence comparison, and domain exchange experiments have demonstrated that the 60- and 66-kDa subunits of human SF3a (SF3a60 and SF3a66) are the mammalian homologues of yeast Prp9p and Prp11p, respectively (Behrens et al., 1993; Bennett & Reed, 1993; Brosi et al., 1993a; Chiara et al., 1994; Krämer et al., 1994). More recently, the isolation of a cDNA for SF3a120 has revealed its homology with the PRP21 protein (Krämer et al., 1995).

In the yeast SF3a complex, Prp21p interacts with both Prp9p and Prp11p, but the latter proteins do not contact each other directly (Legrain & Chapon, 1993; Legrain et al., 1993). The *PRP21* gene has been characterized independently as a heat-sensitive pre-mRNA splicing mutant (Arenas & Abelson, 1993) and as a suppressor of the *prp9-1* mutation (Chapon & Legrain, 1992). Prp9p and Prp11p exhibit structural and functional similarities: both proteins contain zinc finger-like domains that are important for their homodimerization and *prp9-1* and *prp11-1* heat-sensitive mutants are deficient for interaction with Prp21p (Legrain & Choulika, 1990; Legrain & Chapon, 1993; Legrain et al., 1993). However, Prp9p and Prp11p differ by several other criteria: when assayed in an in vivo pre-mRNA nuclear export assay, *prp9-1* but not *prp11-1* exports unspliced mRNAs at the nonpermissive temperature (Legrain & Rosbash, 1989). In addition, these mutants exhibit different spliceosome assembly defects in vitro (Legrain et al., 1993; Ruby et al., 1993; Abovich et al., 1994). The molecular basis of interaction of Prp21p with Prp9p and Prp11p is unknown, and it is not clear whether Prp21p has additional functions related to splicing. Interestingly, Prp21p, its human counterpart, SF3a120, and a homologous protein in *C. elegans* share a common motif with the so-called SWAP proteins (including the *Drosophila* protein *suppressor-of-white-apricot*) that are thought to regulate alternative splicing pathways (Denhez & Lafyatis, 1994; Spikes et al., 1994; Krämer et al., 1995). The homology between Prp21p homologues and SWAP proteins is limited to the two tandemly repeated *surp* modules, and the spacing between the modules differs between Prp21 and SWAP proteins. Given the evolutionary conservation and the role of the SWAP proteins as splicing regulators, it has been proposed that *surp* motifs are essential for interactions with other splicing factors such as RNA or proteins (discussed in Hodges & Beggs, 1994).

A series of heat-sensitive *prp21* mutants was isolated to characterize functional domains of Prp21p and to identify potential additional functions of this protein. Mutant forms of Prp21p were assayed for interactions with Prp9p and Prp11p. *prp21* heat-sensitive mutations were associated with defects in the interaction with Prp9p, but not with Prp11p. These mutants also exhibit splicing defects and export nuclear pre-mRNA at the restrictive temperature. Domains required for viability have been defined by deletion analyses. These domains are responsible for the interaction with Prp9p and Prp11p and are conserved through evolution. Surprisingly, these domains do not include the *surp1* motif, suggesting that this motif might be important for a still unknown function.

RESULTS

Screening of ts PRP21 mutants

The *PRP21* gene encodes a protein of 280 amino acids and is essential for viability (Chapon & Legrain, 1992). To study the effects of *prp21* mutations on growth, a yeast strain, LT1, was constructed in which the chromosomal *PRP21* locus is interrupted and a wild-type copy of the gene is carried on a plasmid with a *URA3*

marker (see the Materials and methods; Fig. 1). *PRP21* open reading frames (ORFs) mutagenized by PCR were cloned in a *TRP1* centromeric plasmid downstream the *PRP21* wild-type promoter sequence. LT1 cells were transformed with this library of *TRP1* plasmids and transformants were cured of the wild-type *PRP21* gene by plating on 5-fluoro-orotic acid-containing plates (5-FOA) (Boeke et al., 1987). Of 500 transformants, 360 grew on 5-FOA plates at 25 °C and were subsequently assayed for growth at various temperatures. Twenty-two heat-sensitive mutants were isolated (4 at 30 °C and 18 at 35 °C), but no cold-sensitive mutants were recovered. Sequence analyses revealed the presence of multiple mutations, ranging from two to nine, within each individual heat-sensitive mutant (Table 1).

Binding of the mutant forms of Prp21p to Prp9p and Prp11p was assayed by subcloning the mutant ORFs into the pGBT9 two-hybrid vector. Interactions with Prp9p and Prp11p were assayed separately at 30 °C (see the Materials and methods; Table 1). Mutants can be grouped according to their binding properties to Prp9p and Prp11p (Fig. 2). Sixteen of 22 mutants display wild-type or increased binding to Prp11p. On the contrary, 18 mutants show decreased or undetectable binding to Prp9p. Only four mutants exhibit normal (or increased) binding activity to Prp9p, and this phenotype is always associated with increased binding to Prp11p. Sequence analyses revealed that these four mutants contain nonsense or frameshift mutations at positions 216, 227, or 240 (see below). Two other *prp21* mutants carry a nonsense mutation at the nearby positions 228 and 230. The accumulation of nonsense mu-

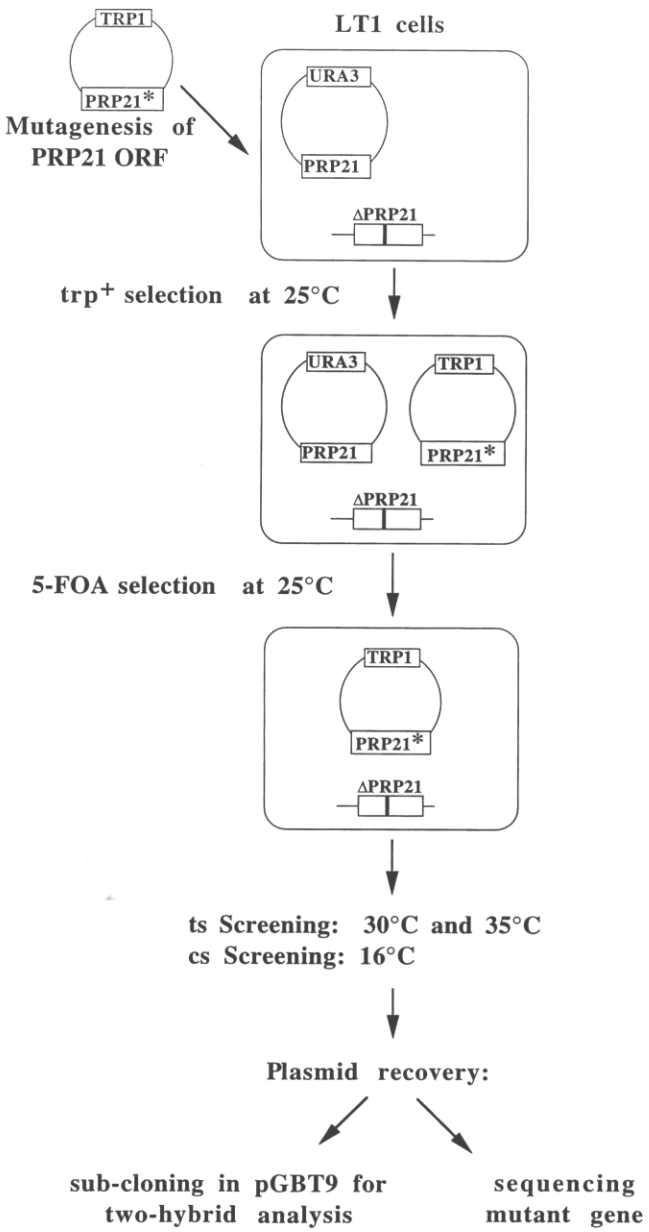

FIGURE 1. Screening of heat-sensitive *PRP21* mutants. The *PRP21* coding sequence was amplified under mutagenic conditions and cloned into a *TRP1* centromeric plasmid. A library of these plasmids was used to transform LT1 yeast cells, which have an interrupted *PRP21* locus and contain a *URA3* plasmid harboring the wild-type *PRP21* gene. After selection of transformants at 25 °C, selection of uracil auxotrophic cells was performed on 5-FOA plates. Patches of yeast cells (or streaked colonies) were then assayed for growth at various temperatures. Plasmid DNA was recovered from heat-sensitive yeast cells and the mutant *PRP21* open reading frame was sequenced and cloned into the two-hybrid pGBT9 vector.

Binding to PRP11 (ß-gal units)

Binding to PRP9 (ß-gal units)	2 - 4	7 - 9	WT 13 - 20	> 25	Total
≤ 2	**4**	**2**	**7**	**1**	14
3 - 5	0	0	**3**	**1**	4
9 - 15 WT	0	0	0	**3**	3
> 25	0	0	0	**1**	1
Total	4	2	10	6	22

FIGURE 2. Binding properties of heat-sensitive PRP21 mutants. The 22 original *PRP21* mutant ORFs were cloned into the pGBT9 vector and protein–protein interactions were assayed in a two-hybrid assay with PRP9 and PRP11 cloned into the pGAD2F vector. β-Galactosidase activity was measured in duplicate for three transformants (Table 1). Wild-type interactions gave 12 and 16 β-galactosidase units for Prp9p and Prp11p binding, respectively. The number of mutants grouped according to their binding to Prp9p and Prp11p is given in the black boxes. The category of mutants with binding properties similar to wild-type Prp21p is designated WT.

TABLE 1. Characteristics of original *prp21* heat-sensitive mutants.[a]

Mutants	Mutations	Growth phenotype	Prp9p binding	Prp11p binding
PRP21	None		12 ± 3	16 ± 4
prp21-1	**C164W**-S218F-D251Y-G262V	30	4	20
prp21-2	K20R-H22Q-E119V*-**Q141R**-Q151H-227Stop	35	11	116
prp21-4	F38Y-H46Q-Y84H-A104T*-E166V-216frameshift	35	9	53
prp21-5	E27G-C164W-K177R-M224V-K254E	30	3	15
prp21-6	T59S-D92G*-K133R-D137E-**T159P**-K177I*-K199N*	30	<0.2	3
prp21-7	D5N-E27A-D137V-E152K-I160N-S218T-230Stop	30	<0.2	19
prp21-12	E111V-**Y142C**-T149I-K154M-T168A-C188G-K240R-K247R-I248V	35	<0.2	2
prp21-16	V16G-D66G-F135L*-D137H*-K189E*-F200L*	35	1	2
prp21-18	**I96N**-E272G*	35	3.6	36
prp21-19	R158T*-E172V-P209S-228Stop	35	1	73
prp21-20	L98S-D106G*-F206C*-T231S-G262D	35	3	18
prp21-22	K20M-T59S-Q83K-I88K-Y102N-Q112L*-E174V-T212A-Q255H	35	<0.2	13
prp21-27	D33G-F38L-K157E-W171R-C188S-L221I-Q252R-K261E-279Stop	35	2	14
prp21-29	K20R-Q21L-I96T*-S128P*-H132Q*-I239N-D251G-261Stop	35	0.5	16
prp21-30	M93T*-E94D-L122S*-K177T*-K199R-I214V-L226R-G271R-E272G	35	1.5	9
prp21-31	**Y142H**-K279R	35	1	18
prp21-32	E32D-T50S-F81C-D92V*-H132L*-F206L	35	<0.2	4
prp21-33	**F135S**-Q202K-D260G-T273A	35	0.5	7
prp21-34	E4G*-F124L*-227Stop	35	15	80
prp21-35	**I160N**-V203E*-R228I	35	2	14
prp21-40	S82P-M113L*-S128P*-K234M	35	1.5	16
prp21-42	D42A*-M125L*-W197R*-240Stop	35	48	27

[a] Mutations are indicated by the position number with the wt and mutant residues on the left and the right side, respectively. Single mutations that lead to a heat-sensitive phenotype are indicated in bold. Single mutations assayed that do not have any detectable growth phenotype are indicated by *. Growth phenotype indicates the lowest temperature tested at which cells do not grow. Mutant ORFs were cloned in the pGBT9 two-hybrid vector and the resulting proteins assayed for interaction with Prp9p and Prp11p expressed from the pGAD2F vector. β-Galactosidase units were measured for at least two independent transformants in duplicate.

tations around position 230 suggests that an essential domain is located upstream of this region, excluding the selection of nonsense mutants located further upstream.

It is remarkable that none of the heat-sensitive mutants exhibits an interaction with Prp9p and Prp11p that is similar to the wild-type protein (Fig. 2). Such behavior could be expected if Prp21p had another essential function, in addition to binding to Prp9p and Prp11p. No such mutant was found among 360 highly mutagenized *PRP21* ORFs tested in the plasmid shuffling assay. Six mutants exhibit a decreased binding to Prp11p (Fig. 2). All of them exhibit a barely detectable binding to Prp9p and their sequences present multiple mutations. These mutants may encode unstable proteins and were not further analyzed.

Point mutations associated with heat sensitivity affect binding to Prp9p and splicing

Several *prp21* mutants were chosen for the construction of single substitution mutants (see the Materials and methods) and four substitutions that are responsible for heat sensitivity were characterized (I96N, F135S, Y142H, C164W; see Fig. 3C). The point mutations are located in the central part of Prp21p, within or downstream of the *surp2* motif (Fig. 3A). The wild-type *PRP21* gene was cloned previously by complementation of the heat-sensitive *prp21-1* mutation (Arenas & Abelson, 1993). We cloned this mutant allele and identified its mutation as a substitution at one of the four residues identified above (C164Y). The binding properties of these mutant proteins were analyzed in the two-hybrid assay at 30 °C. As shown in Figure 3B, all mutant proteins exhibit a decreased binding to Prp9p and a wild-type binding to Prp11p. To learn if the interactions with Prp9p are heat-sensitive, we repeated the two-hybrid assays at 25 °C and 37 °C (Fig. 4). At 25 °C, binding activities to Prp9p are slightly decreased for three mutants (I96N, Y142H, C164W) and more significantly affected for the fourth one (F135S); at 30 °C and 37 °C, the binding of all four to Prp9p is decreased significantly compared to the binding of the wild-type Prp21p. On the contrary, Prp21 mutant proteins bind to Prp11p with an efficiency similar to that of wild-type Prp21p at the three temperatures (Fig. 4). In conclusion, these experiments show that *prp21* mutations affect binding to Prp9p, but not binding to Prp11p, rendering the former interactions heat-sensitive.

The *prp21-34* mutant has three substitutions, E4G, F124L, and a nonsense codon at position 227. Unlike the mutants described above, its binding to Prp9p is

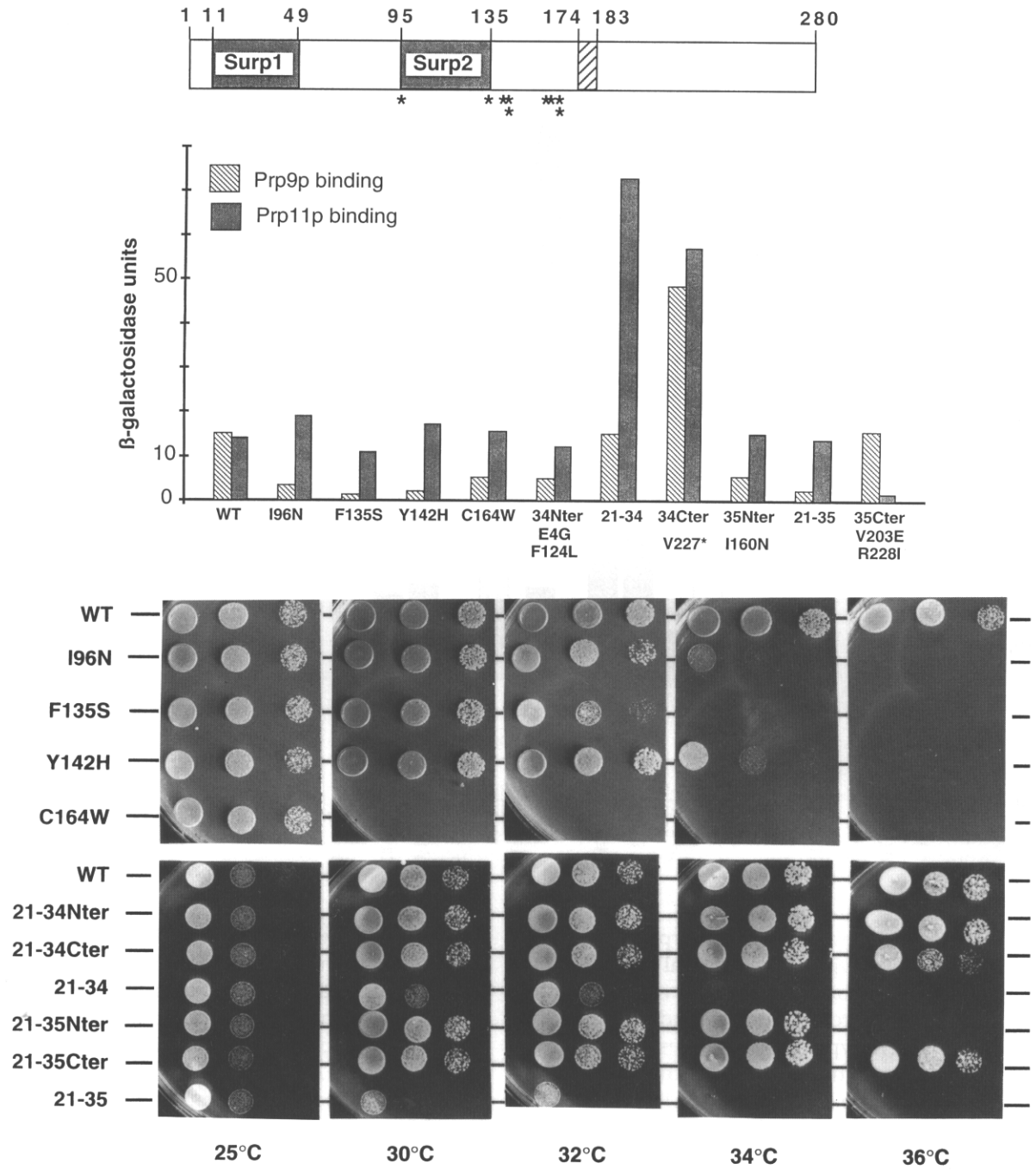

FIGURE 3. Phenotypes of *PRP21* point mutants. **A:** Main structural features of the Prp21 protein are shown. Numbers indicate amino acid positions bordering the individual motifs. Hatched box corresponds to a region of charged amino acids (see Fig. 9). Single mutations that have a heat-sensitive phenotype are indicated by stars (see text). **B:** Wild-type and mutant Prp21 proteins were tested for interactions with Prp9p (hatched) and Prp11p (grey) in a β-galactosidase assay. Transformants were assayed in duplicate (less than 5% variation). Mutants are identified by the position substituted, preceded by the wild-type, and followed by the mutant residue (the original *prp21-34* and *prp21-35* mutants are also indicated). V227* designates a nonsense codon at position 227. **C:** Growth phenotype of *prp21* mutants was analyzed by incubating cells ($5 \cdot 10^4$, $5 \cdot 10^3$, and $5 \cdot 10^2$) at different temperatures for 1–2 days on complete medium. The point mutations of *21-34* and *21-35* mutant derivatives are indicated in Figure 3B. WT, wild-type.

comparable to the wild-type protein, whereas the binding to Prp11p is increased about threefold (Fig. 3B). The single substitution mutant harboring only the nonsense codon (V227*) has a very slight growth phenotype at 36 °C (Fig. 3C), but its interactions with both Prp9p and Prp11p are strongly enhanced compared to the wild-type protein. The mutant containing the two amino acid substitutions exhibits no growth pheno-

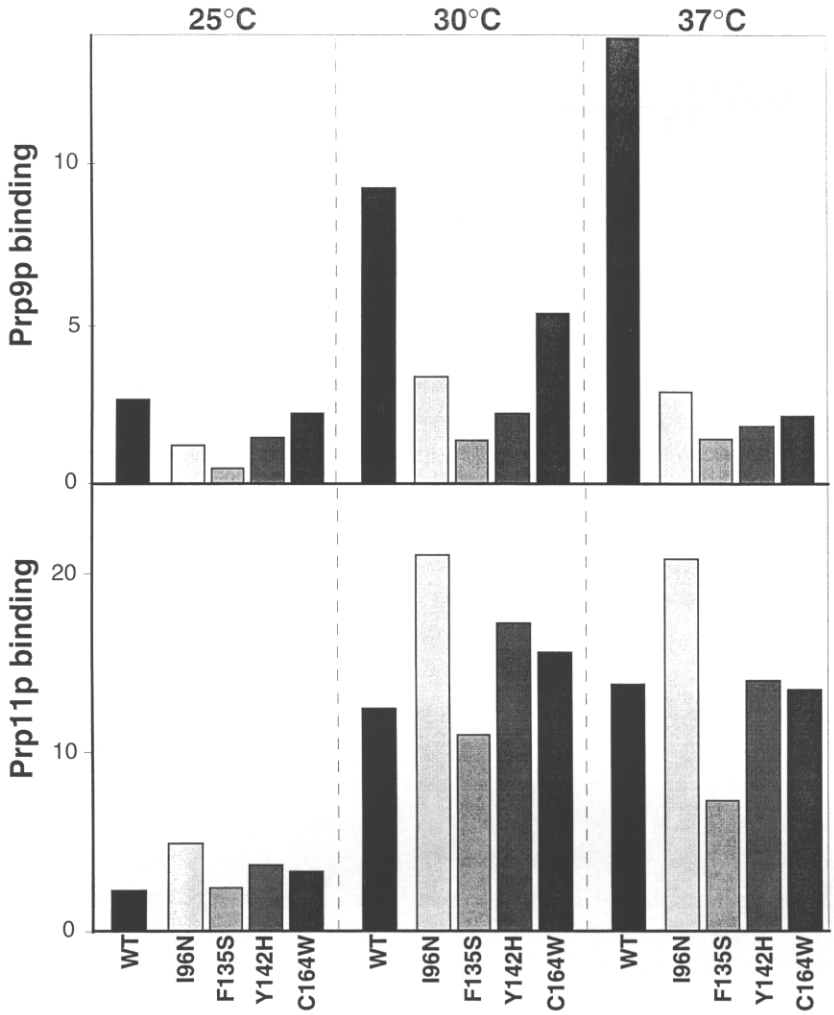

FIGURE 4. Heat-sensitivity of Prp9p–Prp21p mutant interactions. Two-hybrid assays were performed on cells grown at 25°, 30°, or 37 °C. Results are expressed as β-galactosidase units. Measurements were made on three independent transformants in duplicate (less than 5% variation between duplicates).

type, but shows decreased binding to Prp9p. Thus, the heat-sensitive phenotype of the original *prp21-34* mutant arises from the combination of several substitutions, leading to apparently normal binding to Prp9p. Similarly, the phenotype of *prp21-35* results from the combination of mutations affecting the binding to Prp9p (I160N) and the binding to Prp11p (V203E and R228I; the point mutant V203E has similar binding properties, data not shown). The I160N substitution is a weak heat-sensitive mutation (no growth at 36 °C) and the V203E/R228I mutant has no growth phenotype (Fig. 3C).

To identify additional single mutations responsible for heat sensitivity, individual substitutions present in the original 22 ts mutants were tested. Thirty-seven additional mutations were analyzed for their putative growth phenotype (Table 1). Only three mutants did not grow, one at 35 °C (Y142C, at a position already identified by a different substitution), and two at 37 °C (Q141R and T159P; Fig. 3A). The growth phenotypes of mutants at positions Q141 and T159 were associated with a decreased binding to Prp9p (data not shown). Several other mutants exhibited a decreased growth rate at 37 °C (L98S, Y102N, K157E, E172V, C188G). The other 29 mutants (including 13 substitutions in the *surp2* motif) had no detectable growth phenotype (Table 1). Thus, most of the original mutants are heat-sensitive due to the presence of multiple mutations.

In conclusion, these results show that: (1) single mutations responsible for strong growth phenotypes are located in the central part of Prp21p (aa 95–170), outside of the *surp1*, at the extremities of the *surp2* module and downstream from this module (Fig. 3A); (2) these mutations affect binding to Prp9p; (3) binding to Prp11p is decreased by a mutation at position V203, suggesting the existence of independent domains responsible for the binding to Prp9p and Prp11p; (4) the C-terminal domain of Prp21p (aa 227–280) is dispensable for viability of LT1 cells at 25–37 °C, and the resulting truncated proteins exhibit an increased binding to both Prp9p and Prp11p.

Analysis of deletion mutants

To delineate domains in Prp21p that are essential for interactions with Prp9p and Prp11p, a two-hybrid anal-

ysis was performed with N-terminal truncated derivatives of Prp21p (Fig. 5A). PCR-derived fragments of *PRP21* were cloned into the two-hybrid vector pGBT9. N-terminal deletions of increasing sizes decrease binding to Prp9p: the C-terminal fragment spanning amino acids 173–280 displays wild-type binding to Prp11p and no detectable interaction with Prp9p. Larger fragments have more subtle phenotypes: an N-terminal deletion up to the *surp1* motif (fragment 53–280) exhibits a slightly decreased binding to Prp9p and Prp11p; binding is weaker for a more extensive N-terminal truncation (aa 89–280). The removal of the *surp2* motif restores wild-type binding to Prp11p, but shows almost no binding to Prp9p (aa 141–280; Fig. 5A).

Sequences necessary for binding to Prp9p and Prp11p do not extend beyond position 227, because a nonsense mutant at position 227 exhibits strong binding to both Prp9p and Prp11p (Fig. 3B). In addition, a fragment spanning the first 184 N-terminal residues of Prp21p exhibits wild-type binding to Prp9p and no significant binding to Prp11p (Fig. 5B). These results suggested that Prp21p domains involved in binding to Prp9p and Prp11p are located in the central part of the protein and are mostly independent from each other. To confirm this hypothesis, the N-terminal deletions were combined with a C-terminal deletion (aa 1–184) or a nonsense mutation at position 227 and the binding properties of the resulting fragments were analyzed (Fig. 5B). In the absence of the C-terminal last 53 amino acids, binding to Prp11p is independent of the N-terminal region of Prp21p, confirming that the minimal Prp21p sequence necessary for an interaction with Prp11p corresponds to residues 173–227. The decreased binding to Prp11p of Prp21p with N-terminal deletions (aa 89–280; aa 141–280, Fig. 5A) could be caused by incorrect folding of the C-terminal portion of the truncated proteins. Sequences encompassing amino acids 53–184 bind Prp9p as strongly as the C-terminal truncation (1–184), confirming that the binding to Prp9p does not depend upon the first *surp* motif. Moreover,

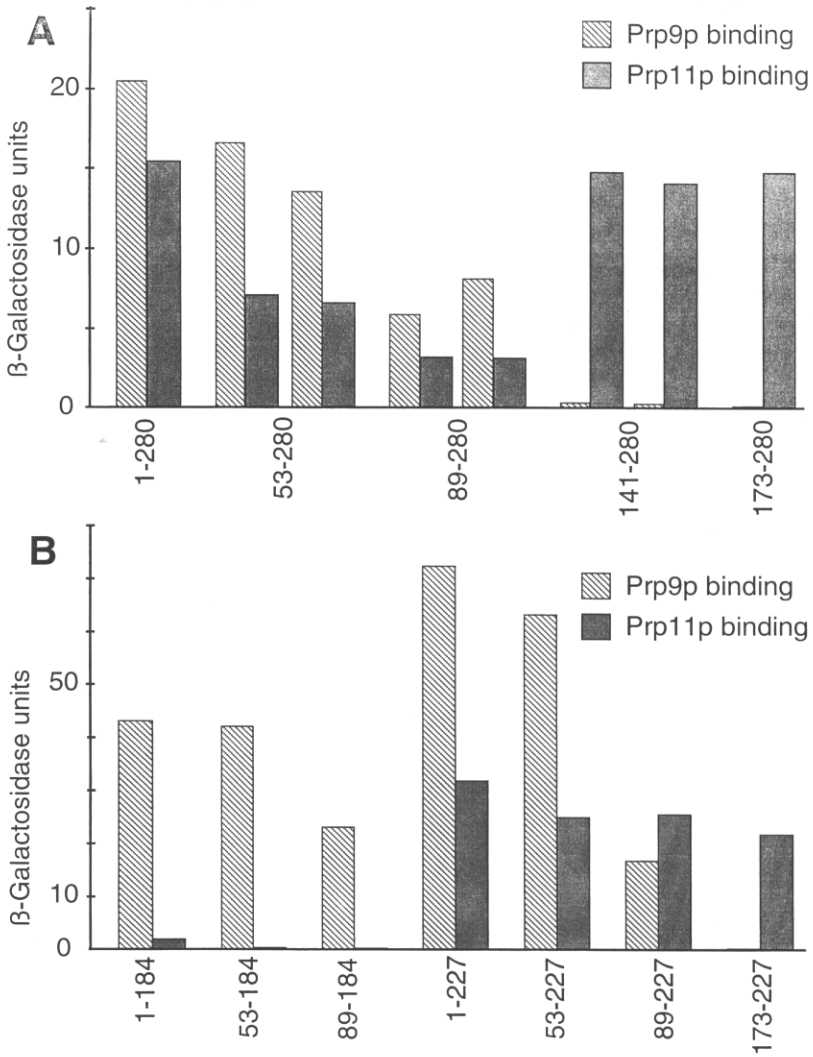

FIGURE 5. Binding of truncated derivatives of Prp21p to Prp9p and Prp11p. Prp9p (hatched) and Prp11p (grey) binding of wild-type Prp21p (1–280) or Prp21p derivatives is presented. Protein fragments are identified by the first and last residues of Prp21p present in the fusion protein. Fragments were cloned after PCR amplification and results for two independent constructs are presented. For each clone, several independent transformants were assayed in duplicate (less than 5% variation between duplicates). **A:** N-terminal truncations. **B:** C-terminal truncations or combinations of N-terminal and C-terminal truncations. Note that the scales on the ordinates are different in A and B.

the smaller fragment (89–184) retains strong binding to Prp9p. Thus, the minimal Prp21p domain necessary for contacts with Prp9p is located between amino acids 89–184. This experiment confirms that Prp21p interacts with Prp9p and Prp11p through two independent domains and that sequences encompassing amino acids 89–184 and 173–227 are sufficient for binding to Prp9p and Prp11p, respectively.

Essential domains of the PRP21 protein

The above results indicate that the N- and C-terminal regions of Prp21p are dispensable for binding to Prp9p and Prp11p. Moreover, no heat-sensitive mutation has been detected in these regions. To investigate whether these parts of Prp21p provide an essential function in vivo, the truncated derivatives of Prp21p were assayed for their ability to support growth. Mutants were cloned into the *TRP1* centromeric vector and assayed by the same strategy that had been used for the screening of heat-sensitive mutants (Fig. 1). No transformant carrying the smallest Prp21p derivative (aa 141–280; lacking the Prp9p interaction domain) could be selected on 5-FOA plates, indicating that this mutant is lethal. Other mutants were viable and growth was assayed at various temperatures (Fig. 6). Strikingly, deletion of the *surp1* motif did not cause a growth phenotype at any temperature (strain B). The mutant deleted up to the region located between the two *surp* motifs was heat-sensitive at 36 °C (strain C). As mentioned above, the nonsense mutation at position 227 exhibited a slight growth phenotype at 36 °C (strain D). The mutant combining the N-terminal deletion with the nonsense mutation (strain E) showed a slight growth phenotype similar to the nonsense mutation alone, and the larger deletion (aa 89–227, strain F) did not grow at 30 °C. This could be due to a partial truncation of the Prp9p interaction domain (see above) or, alternatively, to an overall destabilization of the protein.

In conclusion, N-terminal and C-terminal sequences of Prp21p are dispensable for growth, but the combination of terminal deletions is detrimental for the cells. The essential domains of Prp21p are located in the central part of the protein (aa 90–230) and correspond to the Prp9p and Prp11p binding domains. Other regions of Prp21p may contribute to its stability and optimal folding or, alternatively, may sustain another function that is dispensable under standard growth conditions.

prp21 heat-sensitive mutants exhibit a splicing defect and a pre-mRNA export phenotype

prp9-1 and *prp11-1* heat-sensitive mutants were analyzed previously in a splicing assay and a pre-mRNA export assay (Legrain & Rosbash, 1989). Both mutants were defective for splicing at the nonpermissive temper-

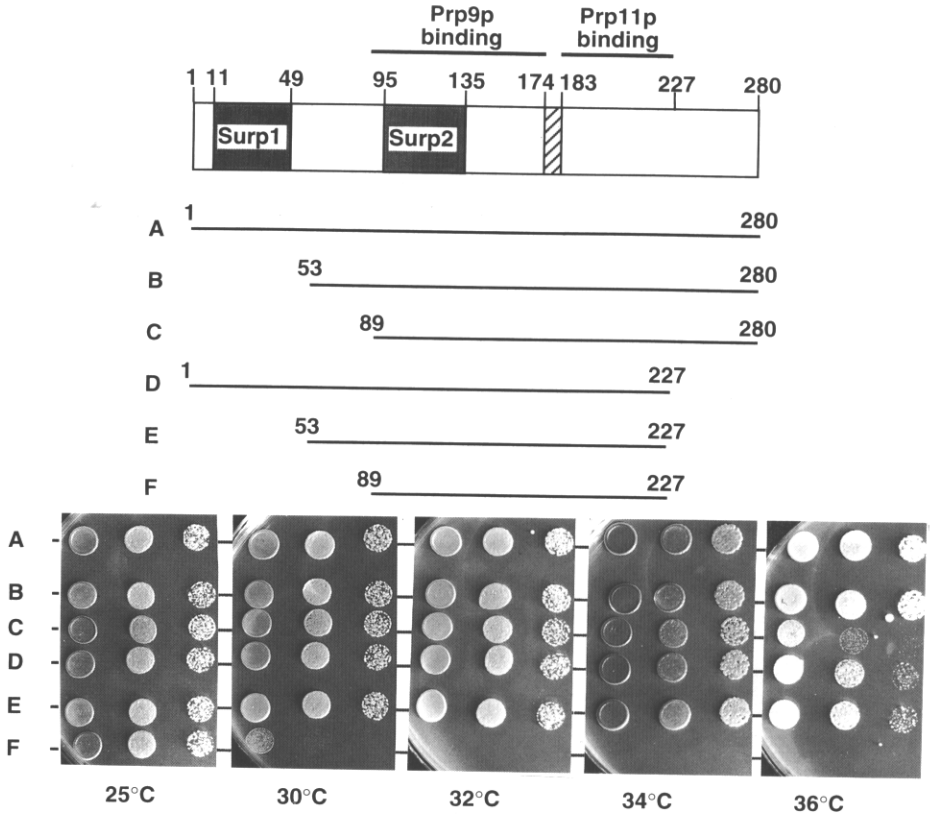

FIGURE 6. Growth phenotypes of *PRP21* deletion mutants. The main features of the Prp21 protein are depicted at the top (see Fig. 3). Minimal fragments required for Prp9p and Prp11p binding are indicated. The extent of wild-type and mutant Prp21 proteins is indicated by the number of their first and last amino acids. The growth phenotype of *prp21* mutants was analyzed by incubating cells ($5 \cdot 10^4$, $5 \cdot 10^3$, and $5 \cdot 10^2$) at different temperatures for 1–2 days on complete medium.

ature, but only *prp9-1* exported pre-mRNA efficiently, suggesting a defect for spliceosome assembly or stability. Potential splicing defects of *prp21* mutants were analyzed similarly using a *lacZ* reporter gene that includes a synthetic intron. This intron is poorly spliced and is a very sensitive reporter for splicing. In addition, a similar construct was used that allows the translation of the pre-mRNA open reading frame to measure the pre-mRNA export to the cytoplasm (Legrain & Rosbash, 1989). Splicing efficiencies and pre-mRNA export were measured at permissive and restrictive temperatures for various mutants (Fig. 7). Several mutants exhibit a poor splicing efficiency, even at permissive temperature, compared to the wild-type strain (21–34, 35Cter, 21–35, I96N, and F135S; Fig. 7A). This result is expected with a very sensitive reporter for splicing activity. All heat-sensitive mutants show a poor splicing activity at 37 °C. Splicing is undetectable for mutants with a se-

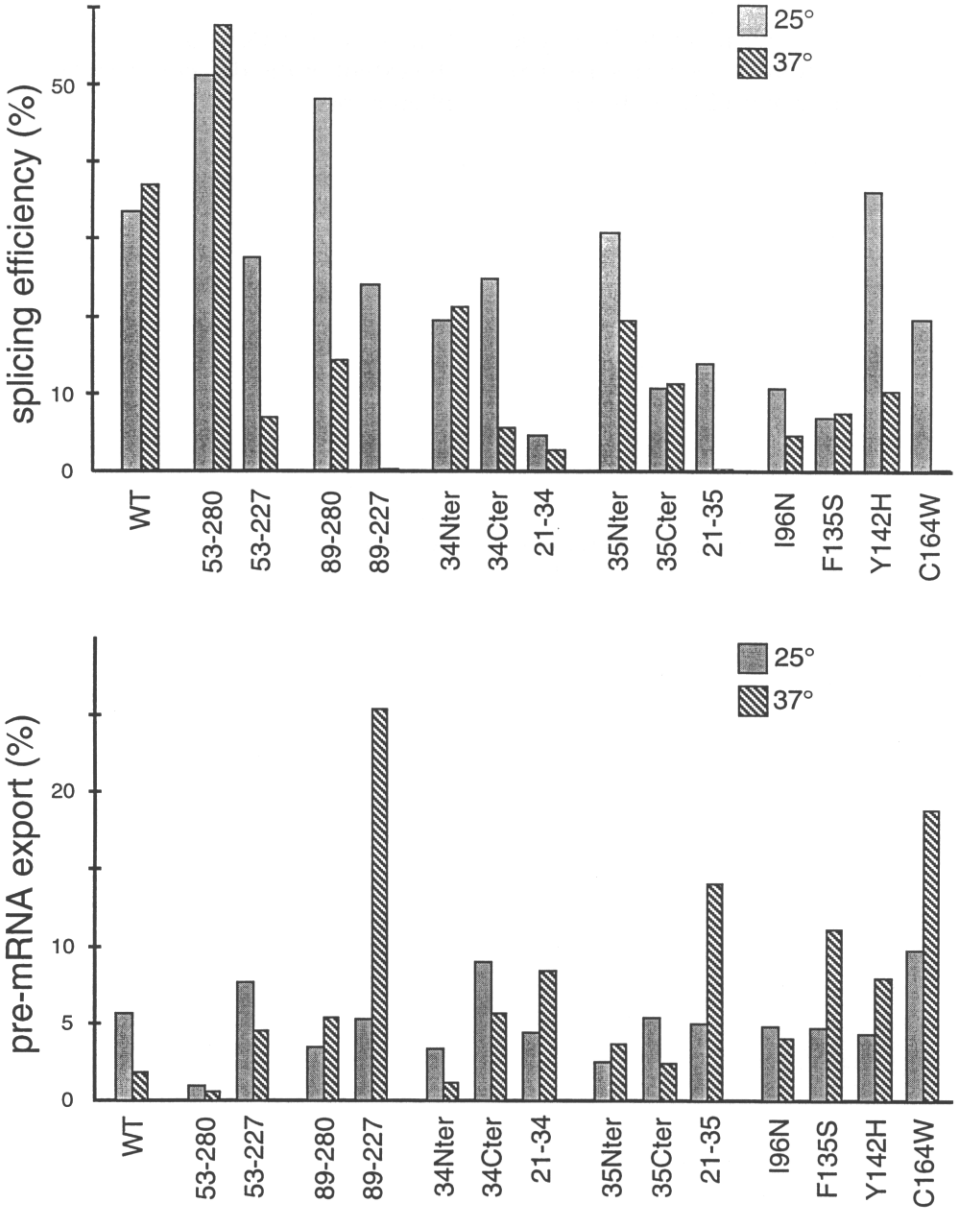

FIGURE 7. Splicing defect and pre-mRNA export of *prp21* mutants. The splicing efficiency (**A**) and the pre-mRNA export (**B**) of various yeast cells were analyzed at 25 °C and 37 °C (see the Materials and methods for details). Deletion mutants are identified by their first and last amino acid residues; 21–34 and 21–35 are composite mutants described in Figure 3. I96N, F135S, Y142H, and C164W are point mutations. Growth phenotypes of *prp21* mutants are presented in Figures 3C and 6. Note that pre-mRNA export at 37 °C in wild-type cells is diminished compared to the export at 25 °C (see also Legrain & Rosbash, 1989; Chapon & Legrain, 1992).

vere growth phenotype (deletion mutant 89–227, 21–35, and C164W), making a clear link between heat sensitivity and splicing defect.

Analysis of pre-mRNA export indicates that the splicing defect of most heat-sensitive *prp21* mutants (with the exception of I96N) correlates with an export of pre-mRNA, as was found originally for the *prp9-1* mutant (Fig. 7B). Mutants with a strong growth phenotype exhibit the strongest export phenotype. Also, for composite mutants (*prp21-34* and *prp21-35*), it should be noted that splicing defect and pre-mRNA export correlate well with growth phenotypes of individual mutations: 34Cter and 35Nter mutants exhibit slight defects, whereas 34Nter and 35Cter do not (Figs. 3C, 7). In conclusion, *prp21* heat-sensitive mutants show splicing defect and export pre-mRNA at the restrictive temperature, confirming the role of Prp21p in the splicing process.

To further characterize the splicing defect of *prp21* mutants, RNA was prepared from cells incubated under permissive or restrictive conditions and analyzed by northern blot with a probe for *RP51A* transcript (Fig. 8). The *RP51A* gene contains an intron that is spliced efficiently under standard growth conditions (Chapon & Legrain, 1992). RNA from heat-sensitive cells (89–227, I96N, F135S, Y142H, and C164W; lanes 14, 16, 18, and 20) incubated at 37 °C do not contain significant amounts of spliced *RP51A* RNA. The four weak deletion mutants (53–280, 89–280, 1–227, and 53–227; lanes 4, 6, 8, and 10) exhibit a decreased amount of spliced RNA compared to the wild-type strain (lane 1). Pre-mRNA molecules are detected in all mutant cells under restrictive conditions, but do not accumulate in large quantities, suggesting that a degradation process occurs. This observation could be related to the active pre-mRNA export observed with a specific *lacZ* reporter (Fig. 7B). The cytoplasmic degradation of pre-mRNA molecules whose intronic sequences contain numerous nonsense codons is very likely and was demonstrated very recently (Long et al., 1995). It should be noted that pre-mRNA molecules accumulate also in the 53–280 deletion mutant at 37 °C, although this mutant exhibits no growth phenotype (Fig. 6).

In conclusion, analysis of splicing defects for a natural intron shows that *prp21* mutants do not splice efficiently pre-mRNAs under restrictive conditions and the extent of the defect is correlated with the growth phenotype.

Heterologous interactions

Human and *C. elegans* homologues of yeast Prp21p (SF3a120 and CePrp21) have been identified recently (Spikes et al., 1994; Krämer et al., 1995). An alignment of the sequences conserved among these proteins is shown in Figure 9. In addition to the *surp1* and *surp2* modules, which are also found in SWAP proteins (Spikes et al., 1994), sequences flanking the *surp2* module and sequences downstream of a stretch of charged residues (aa 193–225 in the yeast protein) are conserved in the Prp21 homologues. These segments correspond to the domains that are required for the interaction of Prp21p

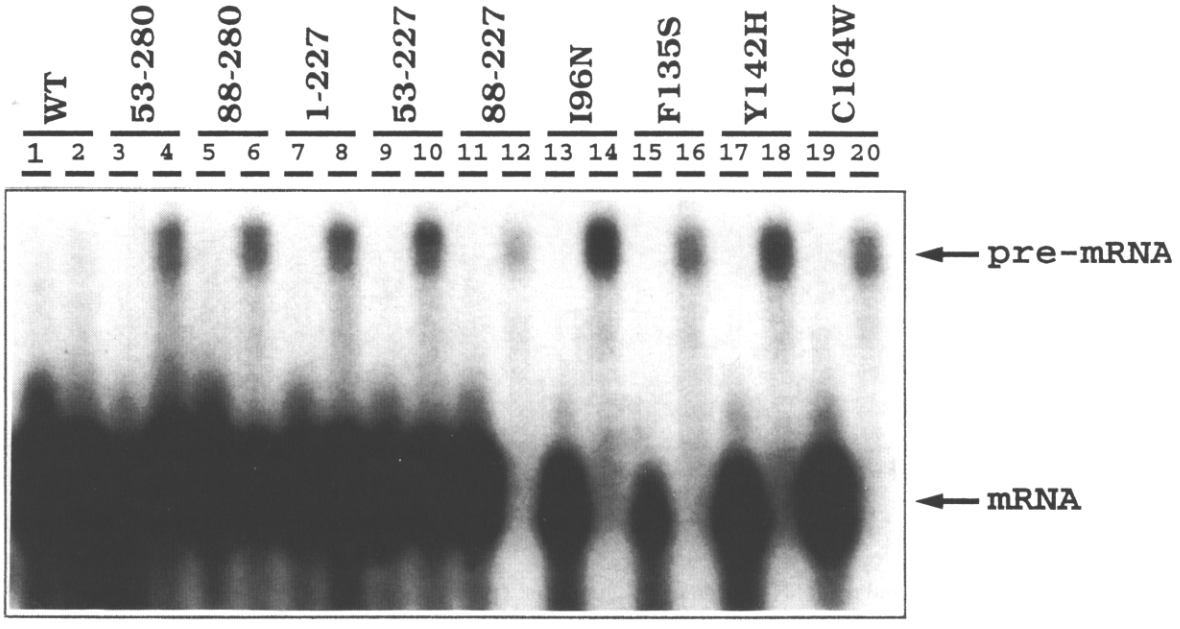

FIGURE 8. Northern blot analysis of unspliced and spliced RNA in mutant *prp21* cells. Total RNA was prepared from cells grown at 25 °C (odd lanes) or incubated at 37 °C (even lanes). Mutant cells are labeled as in Figure 7. The membrane was probed with a DNA fragment detecting *RP51A* transcripts (pre-mRNA and spliced RNA).

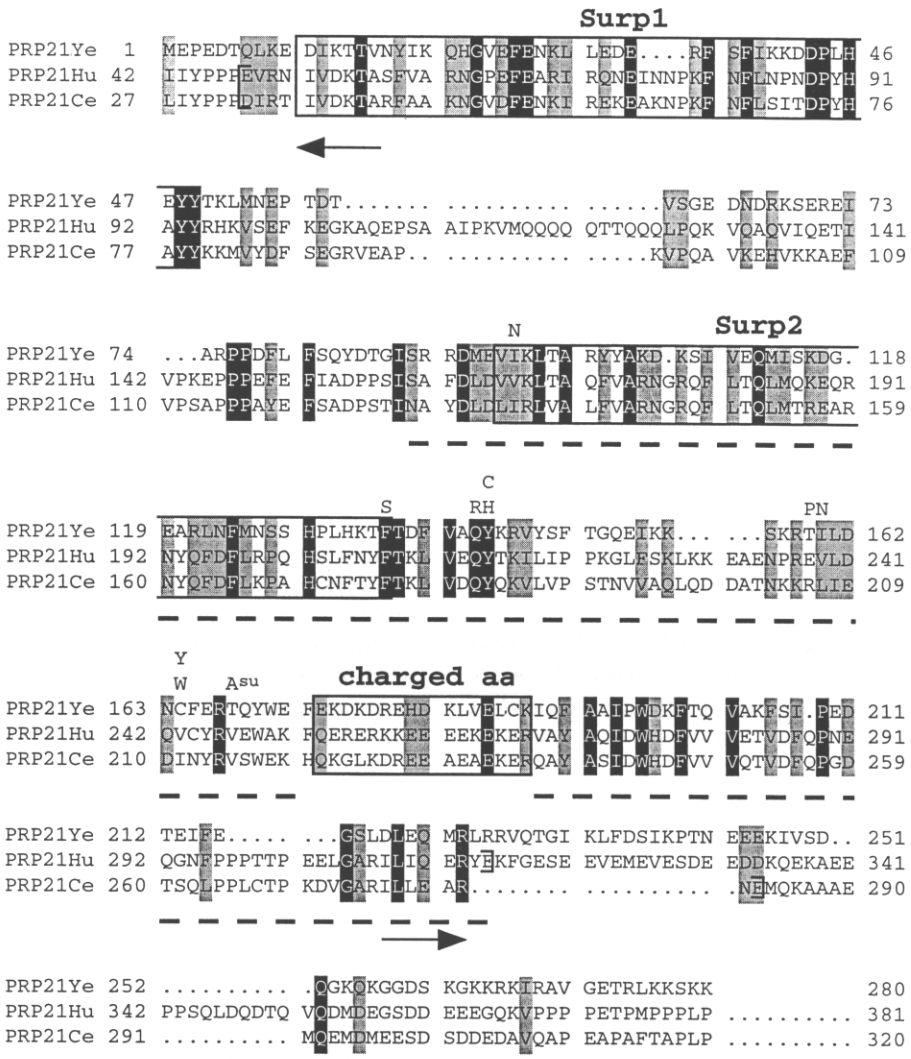

FIGURE 9. Alignment of yeast, human, and nematode Prp21 proteins. The complete sequence of the yeast Prp21 protein is given. Protein sequences were aligned using the Clustal program (Higgins & Sharp, 1989). Identical (black shading) and similar (grey shading) residues among the three proteins are shown. Noticeable structural features are boxed (see text). Point mutations in yeast Prp21p that are associated with a growth phenotype are indicated by the substituted residue above the sequence (see text for details). The following point mutations located in the *surp2* module have no detectable growth phenotype: I96T, A104T, D106G, Q112L, M113L, E119V, L122S, F124L, M125L, S128P, H132Q, H132L, and F135L. The suppressor of the *prp9-1* mutant is indicated by A^{su} (Chapon & Legrain, 1992). Minimal sequences required for binding to Prp9p and Prp11p are indicated by dashed lines (on the N-terminal side and the C-terminal side of the region of charged amino acids, respectively). Fragments of the human and nematode proteins used in the two-hybrid assay are delineated with brackets (they overlap for the region of charged residues). Limits of the human fragment used in the functional complementation assay are indicated by arrows.

with Prp9p and Prp11p, raising the possibility that heterologous interactions between the Prp21p homologues and yeast Prp9p and Prp11p could be detected. Appropriate PCR-derived fragments of the human and nematode cDNAs were therefore cloned into the pACTII two-hybrid vector (Fig. 9; see the Materials and methods). Protein–protein interactions were analyzed with the pAS2 plasmids expressing yeast *PRP9* and *PRP11* (Table 2). A portion of human SF3a120 expected to bind Prp9p shows weak but significant binding to yeast Prp9p, but not to Prp11p, whereas the homologous nematode construct has no detectable binding activity. The putative Prp11p binding domains in the human and nematode proteins interact strongly with yeast Prp11p. The interactions are specific because no binding to yeast Prp9p is detected with these two constructs (Table 2).

We further investigated whether a truncated derivative of human SF3a120 encoding only the two domains expected to bind Prp9p and Prp11p could replace the yeast *PRP21* gene in vivo. A human cDNA fragment corresponding to amino acids 48–313 was cloned into

TABLE 2. Heterologous interactions between fragments of human and nematode Prp21 homologues and yeast Prp9p and Prp11p.[a]

		Prp9	Prp11
Yeast Prp21		32 ± 7	61 ± 1
Human Prp21 (48–268)		1.6 ± 0.6	0[b]
Nematode Prp21 (33–236)		0[b]	0[b]
Human Prp21 (253–315)	A	0[b]	29.5 ± 5
	B	0[b]	33.7 ± 5
Nematode Prp21 (221–283)	A	0[b]	20.3 ± 7
	B	0[b]	19.7 ± 8

[a] Yeast Prp9p and Prp11p were expressed from the pAS2 vector as GAL4 DNA binding-domain fusion proteins. Yeast Prp21p or fragments of homologous proteins were expressed from the pACTII vector as GAL4 activating-domain fusion proteins. Results are expressed in β-galactosidase units. Measurements are performed on at least three transformants in duplicate. Fragments of human and nematode genes were cloned by PCR in the pACTII vector and results using independent PCR products (A, B) are presented.

[b] At background level (below 0.2 unit).

the *TRP1* centromeric vector as a fusion with the first 21 nt of the yeast *PRP21* ORF (Fig. 9; see the Materials and methods). The resulting plasmid was assayed in LT1 cells for its ability to replace the plasmid harboring the wild-type *PRP21* gene. No transformant could be selected on 5-FOA plates, suggesting that a partial human SF3a120 cannot replace its yeast counterpart.

DISCUSSION

The yeast Prp21 splicing factor is the prototype of proteins that contain the tandemly repeated *surp* module. These proteins are grouped in two families, Prp21p homologues (including human SF3a120 and nematode CePrp21) and "SWAP" proteins (including the *Drosophila suppressor-of-white-apricot* protein) that are probably involved in the regulation of alternative splicing pathways (Denhez & Lafyatis, 1994; Spikes et al., 1994). Structural homologies between proteins of the two families are limited to the *surp* modules, whereas similarities among members of the same family extend to several other motifs (Denhez & Lafyatis, 1994; Spikes et al., 1994; Krämer et al., 1995). Given this evolutionary conservation and the role of SWAP proteins, it has been proposed that *surp* modules are essential for constitutive and regulated pre-mRNA splicing (Spikes et al., 1994). However, it is currently unknown whether the *surp* motifs correspond to actual functional domains in these proteins.

The *PRP21* gene is essential and the function of its product can be assessed by a growth assay. By plasmid shuffling (Boeke et al., 1987), we have analyzed a collection of randomly mutagenized PRP21 ORFs as well as N- and C-terminal deletions and combinations of these to characterize functional domains of the Prp21 protein. The smallest part of Prp21p (aa 53–280) that allows wild-type growth excludes the *surp1* module (Fig. 6). Thus, this motif is not essential for viability in yeast. Moreover, heat-sensitive point mutations fall mainly outside the *surp2* module and mutations introduced at several conserved positions in this motif have no phenotype (Table 1; Figs. 3, 9). The Prp21p domain interacting with Prp9p overlaps the *surp2* module, making difficult a distinction between two potentially different functional domains (see below).

A functional redundancy between the two Prp21p *surp* motifs cannot be ruled out. Analyses of point mutants indicate that multiple mutations in various domains of Prp21p lead to a heat-sensitive phenotype (Fig. 3 and data not shown). Similarly, a combination of N-terminal (including the *surp1* module) and C-terminal deletions enhances the heat-sensitivity of the mutant (Fig. 6). Thus, phenotypes of any double mutant in the *surp* modules might be due to a double hit in a single functional domain or, alternatively, to a synergistic effect of mutations affecting two different functions of the protein.

Our study identifies the essential domains of Prp21p as those responsible for the binding to Prp9p and Prp11p (Figs. 3, 5). These domains are located in the central part of the protein (89–184 and 173–227, respectively) and do not overlap with each other in so far as one can judge from the analysis of their interactions in the two-hybrid assay (the fragment 1–164, excluding the region of charged amino acids [174–189], binds Prp9p, data not shown). Heat-sensitive growth phenotypes of point mutants were found associated with decreased binding to Prp9p, but not to Prp11p (Fig. 4). However, combining a mutation that decreases binding to Prp11p with a mutation that affects the binding to Prp9p enhances the heat sensitivity phenotype of this latter mutant (*prp21-35*, Fig. 3), emphasizing the importance of both interactions. The original mutants that exhibit a decreased binding to Prp11p also exhibit a decreased binding to Prp9p. The simplest explanation for this phenotype is a misfolding or an instability of the mutant protein. The inability to isolate heat-sensitive mutants that affect solely binding to Prp11p suggest that this Prp21p domain may be more tolerant of sequence modification. This is also indicated by the ability of human and nematode Prp21p homologous domains to bind strongly the yeast Prp11p (see below).

A region of charged amino acids (residues 174–189; Fig. 9) is present in all three homologous proteins, but the identity of the residues at a given position is not conserved. We favor the hypothesis that the charged region does not participate in the binding to Prp9p or Prp11p, but probably contributes to the flexibility of Prp21p between the two domains by exposing a highly hydrophilic segment.

A splicing defect was observed for all *prp21* mutants (Figs. 7A, 8). In addition, a large pre-mRNA export was measured for most *prp21* heat-sensitive mutants, except for I96N, which is the only point mutant located at the

N-terminal extremity of the *surp2* module (Figs. 7, 8). This result was expected because all *prp21* mutants analyzed so far exhibit a decreased binding to Prp9p, whereas the *prp9-1* mutant exports pre-mRNA and affects Prp21p binding (Legrain & Rosbash, 1989; Legrain et al., 1993). Thus, the Prp9p–Prp21p interaction is the functional target of *prp21* and *prp9-1* mutations. On the contrary, the *prp11-1* mutant does not export pre-mRNA under restrictive conditions (Legrain & Rosbash, 1989). This mutation affects Prp11p–Prp21p interaction, but the *prp11-1* mutant exhibits several genetic differences with the *prp9-1* mutant in vivo and in vitro (Legrain & Chapon, 1993; Ruby et al., 1993; Abovich et al., 1994; P. Legrain, unpubl. obs.). The lack of *prp21* mutants that specifically do not bind Prp11p forbids further comparison between Prp9p–Prp21p and Prp11p–Prp21p interactions.

Analyses of the interactions of yeast Prp9p and Prp11p with human and nematode Prp21p homologues reveal a strong functional homology for the binding domains (Table 2). In addition, the comparison of the sequences identifies several conserved residues: three of seven heat-sensitive residues are identical in all three proteins (Fig. 9), as is the position affecting binding to Prp11p (V203). These results are in very good agreement with binding experiments performed with human SF3a subunits using far-western assays and immunoprecipitations (Krämer et al., 1995); A. Krämer & C. Wersig, unpubl. results): the SF3a60 binding domain covers a sequence starting 20 residues upstream the *surp2* module to the region of charged residues (aa 151–243 in the human protein, Fig. 9) and the SF3a66 binding domain encompasses a sequence of 60 residues downstream the region of charged amino acids (243–304). These sequences correspond to the most conserved regions among the three available sequences, in addition to the *surp1* motif (Fig. 9).

The Prp21p domain required for interaction with Prp9p includes the *surp2* motif, but residues important for the binding to Prp9p are also located outside the module (Fig. 3) and the conservation between yeast and metazoan Prp21p extends into these flanking regions (Fig. 9). In particular, the dipeptide glutamine-tyrosine (QY), which is located downstream from the *surp2* module, is invariant in the three proteins and corresponds to heat-sensitive mutant positions. Taking into account these results and those obtained with the human SF3a subunits (Krämer et al., 1995), we propose that the Prp21p domain interacting with Prp9p is not defined by the *surp2* module, but encompasses sequences that extend to both sides of *surp2*. The highly conserved *surp1* and *surp2* modules in Prp21p and in the SWAP proteins are the only motifs shared between these proteins. They might support an important, as yet unknown function. The *surp1* module is clearly not required for essential interactions in constitutive yeast pre-mRNA splicing; however, the *surp1*, as well as the *surp2* module, could serve as binding sites for factors that regulate splicing and SWAP proteins could compete with Prp21p in the binding of these regulatory factors.

Based on our study, the essential role of the Prp21 splicing factor is to bridge Prp9p and Prp11p, forming the SF3a complex, which is necessary to constitute a functional 17S U2 snRNP. Interactions between SF3a and other components of the U2 snRNP remain to be defined. The present study and previous results suggest that these interactions may involve Prp9p and/or Prp11p rather than Prp21p: based on genetic evidence, an unknown factor may bind to Prp9p in addition to Prp21p (Legrain et al., 1993). Moreover, Prp11p binds to Mud2p, a U1 snRNP-associated polypeptide (Abovich et al., 1994).

Analyses of heterologous interactions with the two-hybrid assay is particularly interesting because it allows an assay for functional conservation through evolution at the level of a protein domain rather than for the whole protein. In this respect, it is similar to a domain exchange experiment, which can be attempted when structural homology is well delineated, as for the zinc finger-like motif of Prp9p (Krämer et al., 1994). By combining a genetic approach to identify mutants with a two-hybrid analysis of protein–protein interactions, we dissected a multifunctional protein into various separate functional domains and have demonstrated the conserved nature of some of them. Similar approaches have been described for other proteins, allowing the identification of novel interactions and characterization of corresponding functional domains (see, for example, Amberg et al., 1995). As a general approach, the assay of interactions between heterologous proteins provides an efficient way to delimit functional domains without requiring full functional complementation of a mutant or a gene disruption. The former approach should be successful more often than the latter. Ultimately, these analyses will lead to a demonstration of a functional role for structural motifs, whose importance is otherwise inferred solely on the basis of sequence alignments.

MATERIALS AND METHODS

Yeast strains and plasmids

Strain LT1, used for plasmid shuffling, was constructed as follows: the diploid strain MGD407 (Chapon & Legrain, 1992) was transformed with a *PRP21::LEU2* DNA fragment represented by a 2,300-nt *Xho* I *PRP21* genomic fragment interrupted at the *Xba* I site by a *LEU2* cassette. Integration at the *PRP21* locus was verified by PCR amplification of the Leu^+ transformants, cells were transformed with the plasmid pPL136 (a derivative of the 2 μm pFL44 vector (Bonneaud et al., 1991) harboring the wild-type *PRP21* gene and the *URA3* marker), and sporulated. Several haploid colonies were isolated and characterized. Further experiments were performed with one of the transformants, LT1 (Mat**a** trp1-289 ade2 arg4

his3-delta1 *PRP21::LEU2* pPL136[*PRP21 URA3*]). Derivatives of the centromeric *TRP1* pFL39 vector (Bonneaud et al., 1991) containing various *PRP21* genes were constructed as follows: *PRP21* gene upstream region (starting at the *Eco*R I site 590-nt upstream the start codon) was amplified by PCR and cloned into pFL39 at the *Eco*R I and *Bam*H I sites to give pPL245. Wild-type *PRP21* ORF was cloned into pPL245 as a *Bam*H I–*Pst* I fragment of the pGBT9-PRP21 derivative (pPL244), giving rise to pPL248. Deletion mutants were obtained by PCR amplification and insertion of the corresponding fragments using the same restriction sites. Single substitution mutants were obtained from original mutants, taking advantage of a unique *Nco* I site in the *PRP21* coding sequence (aa 196–197) and a unique *Nde* I site upstream of the *PRP21* gene in the pPL245 derivatives. This strategy allowed the replacement of a fragment of the mutant by the wild-type sequence. Combinations of N-terminal deletions with the nonsense mutation at position 227 were obtained by the same strategy. Site-directed mutagenesis was performed using standard procedures on an SK^+ (Stratagene) derivative encoding the *PRP21* ORF (pPL247).

Screening for heat-sensitive mutants and growth assays

The *PRP21* ORF was amplified by PCR using pPL247 as DNA source and KS and SK primers (Stratagene) under the following mutagenic conditions: 7 mM $MgCl_2$, 0.5 mM $MnCl_2$, 0.2 mM dGTP and dATP, 1 mM dCTP and dTTP (Cadwell & Joyce, 1992). *Bam*H I–*Pst* I fragments were then cloned into pPL245. The plasmid-shuffling strategy is depicted in Figure 1. Patches of transformants were streaked on synthetic complete (SC) medium lacking tryptophan (trp) and grown at 25 °C. Patches were replica-plated on SC-trp once and subsequently replicated twice on 5-FOA plates to select for cells cured of the *URA3* plasmid. Cells that grew on 5-FOA plates were replica-plated or streaked on rich-medium plates and their growth was measured at different temperatures. Growth phenotypes were analyzed by incubating cells ($5 \cdot 10^4$, $5 \cdot 10^3$, and $5 \cdot 10^2$) at different temperatures for 1–2 days on complete medium.

Two-hybrid assays

Two-hybrid assays were performed in the Y526 strain, using pGBT9, pGAD2F, pAS2, and pACTII vectors and derivatives (Fields & Song, 1989; Bartel et al., 1993; Durfee et al., 1993; Harper et al., 1993; Legrain et al., 1994). Qualitative β-galactosidase assays were performed as filter assays directly on transformation plates. Several transformants were streaked and quantitative assays were performed in liquid cultures (Transy & Legrain, 1995). Two-hybrid assays performed on transformation plates with the pGAD2F/pGBT9 combinations gave similar results for all transformants. For the pAS2/pACTII combinations, a minority of fast-growing colonies was observed that always gave negative results in the filter assay (especially with Prp11p constructs, which are toxic and favor plasmid recombinations). These transformants were not analyzed further and only colonies representative of other transformants were streaked and used in the quantitative assay. Cells were grown in liquid culture at 30 °C except when specified. Independent transformants (three in most cases) were assayed for each combination and each culture was assayed in duplicate. Less than 5% deviation was found between duplicates and variation between transformants was within a 30% deviation.

Splicing and pre-mRNA export assays

Splicing efficiency and pre-mRNA export were analyzed in a *lacZ* reporter assay described previously (Legrain & Rosbash, 1989). LT1-derivative cells corresponding to the various prp21 mutants were transformed with plasmids encoding a *lacZ* gene. The control plasmid contains a gene without intron; the splicing reporter is a gene with a synthetic intron whose spliced transcript encodes the β-galactosidase protein; the pre-mRNA export reporter is a similar construct for which the unspliced transcript encodes the β-galactosidase enzyme. These genes are under a galactose-inducible promoter. Cells are grown in the absence of galactose and β-galactosidase activity is measured 1, 2, and 3 h after galactose induction. Splicing efficiency and pre-mRNA export are expressed as the ratio of β-galactosidase activity measured for these reporters to the non-intron containing reporter. Results are presented for the 3-h time point. For measurements under restrictive conditions, cells were grown at 25 °C and shifted to 37 °C by a twofold dilution with pre-heated medium 30 min before galactose induction. All measurements were made for two independent transformants in parallel and duplicates were within 10% variation.

Northern blot

Cells were grown at 25 °C or shifted at 37 °C for 7 h. Growth rate curves indicated that all heat-sensitive mutants had stopped growing at this point (data not shown). Total RNA was prepared according to a standard protocol (Chapon & Legrain, 1992) and blotted onto a N^+ nylon membrane (Amersham, France). An *RP51A* probe was used for pre-mRNA analysis (Chapon & Legrain, 1992). The various RNA preparations were quantified for their mRNA content using a hybridization with a *MUD2* probe, a highly expressed gene without intron (data not shown) (Abovich et al., 1994). The membrane was exposed with a X-OMAT film (Kodak), using an intensifying screen.

Heterologous proteins

The nematode cDNA encoding CePrp21 (Spikes et al., 1994), obtained from K. van Doren, and the human SF3a120 cDNA (Krämer et al., 1995) were used for PCR amplification and cloned into the pACTII vector as *Nco* I–*Xho* I and *Nco* I–*Bam*H I fragments for the N- and C-terminal regions, respectively. Sequences were verified after cloning. The human cDNA was digested with *Ssp* I (Biolabs) and *Eco*47 III (Fermentas), leading to a DNA fragment with blunt ends (encoding amino acids 52–313). This fragment was cloned into pPL248 that had been cut with *Pst* I, digested partially with *Pvu* II, and blunted with T4 DNA polymerase. The junctions of the resulting clone were controlled by sequencing. This construct encodes the following fusion protein: MEPEDTQ . . . human aa 52–313 . . . HASLA.

ACKNOWLEDGMENTS

We thank K. van Doren and J. Arenas for providing the nematode PRP21 cDNA and the yeast *prp21-1* strain, respectively. A. Rose contributed to some experiments during a training course as a technician (IUT, Nancy). This work was initiated in the laboratory of B. Dujon and we thank him for support. We are particularly indebted to C. Chapon and C. Transy for many stimulating discussions. We are grateful to A. Jacquier, G. Chanfreau, and M. Fromont for continuous interest in this work, many useful suggestions, and critical reading of the manuscript. This work was supported in part by the Fondation de la Recherche Médicale, by the CEC contract CHRX-CT94-0677 to P.L., and by ACS grant VM-131 and NIH grant GM46569 to A.M.T. during his sabbatical year at the Pasteur Institute.

Received October 29, 1995; returned for revision December 21, 1995; revised manuscript received April 5, 1996

REFERENCES

Abovich N, Legrain P, Rosbash M. 1990. The yeast PRP6 gene encodes a U4/U6 small nuclear ribonucleoprotein particle (snRNP) protein, and the PRP9 gene encodes a protein required for U2 snRNP binding. *Mol Cell Biol 10*:6417–6425.

Abovich N, Liao XC, Rosbash M. 1994. The yeast MUD2 protein: An interaction with PRP11 defines a bridge between commitment complexes and U2 snRNP addition. *Genes & Dev 8*:843–854.

Amberg DC, Basart E, Botstein D. 1995. Defining protein interactions with yeast actin in vivo. *Nature Struct Biol 2*:28–35.

Arenas J, Abelson J. 1993. The *Saccharomyces cerevisiae* PRP21 gene product is required for pre-spliceosome assembly. *Proc Natl Acad Sci USA 90*:6771–6775.

Bartel PL, Chien CT, Sternglanz R, Fields S. 1993. Using the two-hybrid system to detect protein–protein interactions. In: Hartley DA, eds. *Cellular interactions in development: A practical approach*. Oxford: Oxford University Press. pp 153–179.

Behrens SE, Galisson F, Legrain P, Lührmann R. 1993. Evidence that the 60-KDa protein of the 17S U2 small nuclear ribonucleoprotein particle is immunologically and functionally related to the yeast PRP9 splicing factor and is required for the efficient formation of the prespliceosome. *Proc Natl Acad Sci USA 90*:8229–8233.

Behrens SE, Lührmann R. 1991. Immunoaffinity purification of a [U4/U6·U5] tri-snRNP from human cells. *Genes & Dev 5*:1439–1452.

Bennett M, Michaud S, Kingston J, Reed R. 1992. Protein components specifically associated with prespliceosome and spliceosome complexes. *Genes & Dev 6*:1986–2000.

Bennett M, Reed R. 1993. Correspondence between a mammalian spliceosome component and an essential yeast splicing factor. *Science 262*:105–108.

Boeke JD, Trueheart J, Natsoulis G, Fink GR. 1987. 5-Fluoro-orotic acid as a selective agent in yeast molecular genetics. *Methods Enzymol 154*:164–175.

Bonneaud N, Ozier-Kalogeropoulos O, Li G, Labouesse M, Minvielle-Sebastia L, Lacroute F. 1991. A family of low and high copy replicative, integrative and single-strand *S. cerevisiae*/*E. coli* shuttle vectors. *Yeast 7*:609–615.

Brosi R, Gröning K, Behrens SE, Lührmann R, Krämer A. 1993a. Interaction of mammalian splicing factor SF3a with U2 snRNP and relation of its 60-kD subunit to yeast PRP9. *Science 262*:102–105.

Brosi R, Hauri HP, Krämer A. 1993b. Separation of splicing factor SF3 into two components and purification of SF3a activity. *J Biol Chem 268*:17640–17646.

Cadwell RC, Joyce GF. 1992. Randomization of genes by PCR mutagenesis. *PCR Methods Appl 2*:28–33.

Champion-Arnaud P, Reed R. 1994. The prespliceosome components SAP49 and SAP145 interact in a complex implicated in tethering U2 snRNP to the branch site. *Genes & Dev 8*:1974–1983.

Chapon C, Legrain P. 1992. A novel gene, spp91-1, suppresses the splicing defect and the pre-messenger-RNA nuclear export in the prp9-1 mutant. *EMBO J 11*:3279–3288.

Chiara MD, Champion-Arnaud P, Buvoli M, Nadal-Ginard B, Reed R. 1994. Specific protein–protein interactions between the essential mammalian spliceosome-associated proteins SAP 61 and SAP114. *Proc Natl Acad Sci USA 91*:6403–6407.

Denhez F, Lafyatis R. 1994. Conservation of regulated alternative splicing and identification of functional domains in vertebrate homologs to the *Drosophila* splicing regulator, *suppressor-of-white-apricot*. *J Biol Chem 269*:16170–16179.

Durfee T, Becherer K, Chen PL, Yeh SH, Yang Y, Kilburn A, Lee WH, Elledge SJ. 1993. The retinoblastoma protein associates with the protein phosphatase type 1 catalytic subunit. *Genes & Dev 7*:555–569.

Fields S, Song OK. 1989. A novel genetic system to detect protein–protein interactions. *Nature 340*:245–246.

Harper JW, Adami GR, Wei N, Keyomarsi K, Elledge SJ. 1993. The p21 Cdk-interacting protein Cip1 is a potent inhibitor of G1 cyclin-dependent kinases. *Cell 75*:805–816.

Higgins DG, Sharp PM. 1989. Fast and sensitive multiple sequence alignments on a microcomputer. *CABIOS 5*:151–153.

Hodges PE, Beggs JD. 1994. U2 fulfils a commitment. *Curr Biol 4*: 264–267.

Krämer A, Legrain P, Mulhauser F, Gröning K, Brosi R, Bilbe G. 1994. Splicing factor SF3a60 is the mammalian homologue of PRP9 of *S. cerevisiae*: The conserved zinc finger-like motif is functionally exchangeable in vivo. *Nucleic Acids Res 22*:5223–5228.

Krämer A, Mulhauser F, Wersig C, Gröning K, Bilbe G. 1995. Mammalian splicing factor SF3a120 represents a new member of the SURP family of proteins and is homologous to the essential splicing factor PRP21p of *Saccharomyces cerevisiae*. *RNA 1*:260–272.

Krämer A, Utans U. 1991. Three protein factors (SF1, SF3 and U2AF) function in pre-splicing complex formation in addition to snRNPs. *EMBO J 10*:1503–1509.

Legrain P, Chanfreau G. 1994. Pre-mRNA splicing: From intron recognition to catalysis. *Bull Inst Pasteur 92*:153–179.

Legrain P, Chapon C. 1993. Interaction between PRP11 and SPP91 yeast splicing factors and characterization of a PRP9–PRP11–SPP91 complex. *Science 262*:108–110.

Legrain P, Chapon C, Galisson F. 1993. Interactions between PRP9 and SPP91 splicing factors identify a protein complex required in prespliceosome assembly. *Genes & Dev 7*:1390–1399.

Legrain P, Choulika A. 1990. The molecular characterization of PRP6 and PRP9 yeast genes reveals a new cysteine/histidine motif common to several splicing factors. *EMBO J 9*:2775–2781.

Legrain P, Dokhelar MC, Transy C. 1994. Detection of protein–protein interactions using different vectors in the two-hybrid system. *Nucleic Acids Res 22*:3241–3242.

Legrain P, Rosbash M. 1989. Some *cis*- and *trans*-acting mutants for splicing target pre-mRNA to the cytoplasm. *Cell 57*:573–583.

Legrain P, Seraphin B, Rosbash M. 1988. Early commitment of yeast pre-mRNA to the spliceosome pathway. *Mol Cell Biol 8*:3755–3760.

Long RM, Elliott DJ, Stutz F, Rosbash M, Singer RH. 1995. Spatial consequences of defective processing of specific yeast mRNAs revealed by fluorescent in situ hybridization. *RNA 1*:1071–1078.

Madhani HD, Guthrie C. 1994. Dynamic RNA–RNA interactions in the spliceosome. *Annu Rev Genet 28*:1–26.

Moore MJ, Query CC, Sharp PA. 1993. Splicing of precursors to messenger RNAs by the spliceosome. In: Gesteland R, Atkins J, eds. *The RNA world*. Cold Spring Harbor, New York: Cold Spring Harbor Laboratory Press. pp 303–357.

Ruby SW, Chang TH, Abelson J. 1993. Four yeast spliceosomal proteins (PRP5, PRP9, PRP11, and PRP21) interact to promote U2 snRNP binding to pre-mRNA. *Genes & Dev 7*:1909–1925.

Rymond BC, Rosbash M. 1992. Yeast pre-mRNA splicing. In: Jones EW, Pringle JR, Broach JR, eds. *The molecular and cellular biology of the yeast Saccharomyces*. Cold Spring Harbor, New York: Cold Spring Harbor Laboratory Press. pp 143–192.

Seraphin B, Rosbash M. 1989. Identification of functional U1 snRNA-pre-mRNA complexes committed to spliceosome assembly and splicing. *Cell 59*:349–358.

Seraphin B, Rosbash M. 1991. The yeast branchpoint sequence is not required for the formation of a stable U1 snRNA-pre-mRNA complex and is recognized in the absence of U2 snRNA. *EMBO J 10*:1209–1216.

Spector DL. 1993. Macromolecular domains within the cell nucleus. *Annu Rev Cell Biol 9*:265–315.

Spikes DA, Kramer J, Bingham PM, Van Doren K. 1994. SWAP pre-mRNA splicing regulators are a novel, ancient protein family sharing a highly conserved sequence motif with the prp21 family of constitutive splicing factors. *Nucleic Acids Res 22*:4510–4519.

Transy C, Legrain P. 1995. The two-hybrid: An in vivo protein–protein interaction assay. *Mol Biol Rep 21*:119–127.

Utans U, Behrens SE, Lührmann R, Kole R, Krämer A. 1992. A splicing factor that is inactivated during in vivo heat shock is functionally equivalent to the [U4/U6·U5] triple snRNP-specific proteins. *Genes & Dev 6*:631–641.

Wells SE, Ares MJ. 1994. Interactions between highly conserved U2 small nuclear RNA structures and Prp5p, Prp9p, Prp11p, and Prp21p proteins are required to ensure integrity of the U2 small nuclear ribonucleoprotein in *Saccharomyces cereviae*. *Mol Cell Biol 14*:6337–6349.

Wells SE, Neville M, Haynes M, Wang J, Igel H, Ares M. 1996. CUS1, a suppressor of cold sensitive U2 snRNA mutations, is a novel yeast splicing factor homologous to human SAP145. *Genes & Dev 10*:220–232.

Yan D, Ares M. 1995. Invariant U2 RNA sequences bordering the branchpoint recognition region are essential for interaction with yeast SF3a and SF3b subunits. *Mol Cell Biol 16*:818–828.